DSCAM promotes axon fasciculation and growth in the developing optic pathway

Freyja M. Bruce[a,1], Samantha Brown[a,1], Jonathan N. Smith[a], Peter G. Fuerst[b,c,2], and Lynda Erskine[a,2]

[a]School of Medicine, Medical Sciences, and Nutrition, Institute of Medical Sciences, University of Aberdeen, Aberdeen AB25 2ZD, United Kingdom; [b]Department of Biological Sciences, University of Idaho, Moscow, ID 83844; and [c]Washington, Wyoming, Alaska, Montana, and Idaho (WWAMI) Medical Education Program, University of Idaho, Moscow, ID 83844

Edited by Shanthini Sockanathan, Johns Hopkins University, Baltimore, MD, and accepted by Editorial Board Member Jeremy Nathans December 30, 2016 (received for review November 11, 2016)

Although many aspects of optic pathway development are beginning to be understood, the mechanisms promoting the growth of retinal ganglion cell (RGC) axons toward visual targets remain largely unknown. Down syndrome cell adhesion molecule (*Dscam*) is expressed by mouse RGCs shortly after they differentiate at embryonic day 12 and is essential for multiple aspects of postnatal visual system development. Here we show that *Dscam* is also required during embryonic development for the fasciculation and growth of RGC axons. *Dscam* is expressed along the developing optic pathway in a pattern consistent with a role in regulating RGC axon outgrowth. In mice carrying spontaneous mutations in *Dscam* (*Dscam*^{del17}; *Dscam*^{2J}), RGC axons pathfind normally, but growth from the chiasm toward their targets is impaired, resulting in a delay in RGC axons reaching the dorsal thalamus compared with that seen in wild-type littermates. Conversely, *Dscam* gain of function results in exuberant growth into the dorsal thalamus. The growth of ipsilaterally projecting axons is particularly affected. Axon organization in the optic chiasm and tract and RGC growth cone morphologies are also altered in *Dscam* mutants. In vitro DSCAM promotes RGC axon growth and fasciculation, and can act independently of cell contact. In vitro and in situ DSCAM is required both in the RGC axons and in their environment for the promotion of axon outgrowth, consistent with a homotypic mode of action. These findings identify DSCAM as a permissive signal that promotes the growth and fasciculation of RGC axons, controlling the timing of when RGC axons reach their targets.

axon guidance | development | growth cone | optic chiasm | visual system

The developing vertebrate visual system has proven to be one of the most informative model systems for studying axon growth and guidance decision (1). In mice, retinal ganglion cell (RGC) axons grow into the brain from embryonic day (E) 12.5, although mapping within visual targets is not complete until postnatal stages (1). Molecules have been identified that are important for multiple aspects of RGC axon growth and pathfinding, including guidance out of the eye, constraining the general path followed by RGC axons and midline routing at the optic chiasm underlying the establishment of stereovision (1); however, the majority of these molecules induce inhibitory responses in RGC axons. Much less is known about the growth-promoting mechanisms that drive RGC axon extension.

Down syndrome cell adhesion molecule 1 (Dscam1) is a homophilic adhesion molecule essential for multiple aspects of neural circuit formation in *Drosophila*, including axon growth, fasciculation, and pathfinding; dendritic field organization; and synaptic specificity and targeting (2, 3). Although vertebrate *Dscam* lacks the extensive alternative splicing of fly *Dscam1*, it is required for many of the same developmental processes, including dendritic arborization and synaptic lamination and refinement (4).

Dscam is expressed by mouse RGCs from E12.5 (5) and, through regulation of cell death and homophilic antiadhesive interactions, controls the mosaic spacing and dendritic arborization of RGCs in the postnatal retina (5–7). However, the expression of *Dscam* in RGCs from early embryonic stages raises the possibility that DSCAM may facilitate additional aspects of RGC development, such as controlling axon outgrowth. In support of this idea, DSCAM has been implicated as a receptor for the guidance cue netrin-1 (8, 9), a key factor in controlling the growth of RGC axons out of the eye (10); however, in mice lacking *Dscam*, netrin-dependent guidance of spinal commissural axons occurs normally, arguing against a critical role for DSCAM in axon patterning in vivo (11).

Using two different *Dscam* mutant alleles and mice overexpressing *Dscam* (7), we have found that DSCAM is not essential for the netrin-dependent process of exiting the eye but is expressed along the developing optic pathway, promoting axon fasciculation and providing growth-promoting interactions that help drive RGC axon growth toward visual targets.

Results and Discussion

***Dscam* Is Expressed Along the Developing Optic Pathway.** From E12.5 through to postnatal ages *Dscam* is expressed strongly by most, if not all, RGCs (5). Double immunofluorescent staining of cultured P0 retinal ganglion cells with antibodies validated previously against DSCAM (12–14) and neurofilament confirmed that DSCAM localized to retinal axons, with expression concentrated at the growth cone (Fig. 1*A*, white arrowhead). *Dscam* is also expressed along the developing optic pathway (Figs. 1*B* and Fig. S1). At E12.5, *Dscam* was expressed around the region where the optic nerves join with the brain, posterior to the developing optic chiasm and bordering the presumptive optic tracts (Fig. 1*B*). As development proceeded, the level of *Dscam* increased, and by E17.5, expression was present throughout the ventral

Significance

Our findings demonstrate a function for Down syndrome cell adhesion molecule (DSCAM) in the embryonic development of the mouse visual system. We found that DSCAM promotes fasciculation and growth of axons in the developing mouse optic pathway, at least in part, through homotypic interactions. We also found that shed DSCAM can act independently of direct cell–cell contact to provide growth-promoting signals. Because the *Dscam* mutant phenotypes are mediated in a dose-dependent manner, these results are potentially relevant to human Down syndrome, in which *Dscam* is overexpressed as a result of trisomy of chromosome 21, and fragile-X syndrome, in which *Dscam* is overexpressed because of misregulation of *Dscam* mRNA.

Author contributions: F.M.B., S.B., P.G.F., and L.E. designed research; F.M.B., S.B., J.N.S., P.G.F., and L.E. performed research; P.G.F. and L.E. contributed new reagents/analytic tools F.M.B., S.B., J.N.S., P.G.F., and L.E. analyzed data; and F.M.B., S.B., P.G.F., and L.E. wrote the paper.

The authors declare no conflict of interest.

This article is a PNAS Direct Submission. S.S. is a Guest Editor invited by the Editorial Board.

Freely available online through the PNAS open access option.

[1]F.M.B. and S.B. contributed equally to this work.

[2]To whom correspondence may be addressed. Email: fuerst@uidaho.edu or l.erskine@abdn.ac.uk.

This article contains supporting information online at www.pnas.org/lookup/suppl/doi:10.1073/pnas.1618606114/-/DCSupplemental.

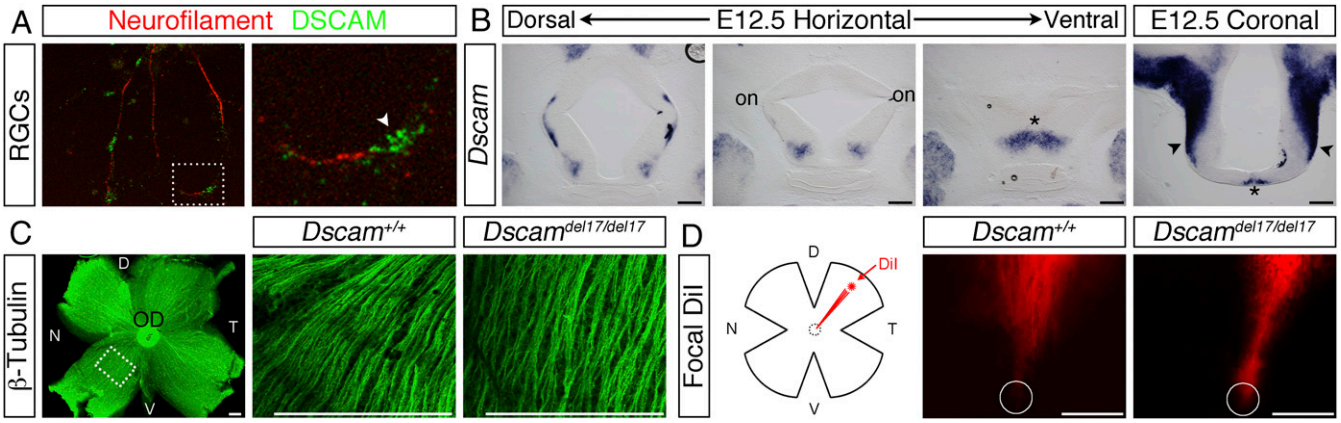

Fig. 1. DSCAM is expressed by retinal axons and along the developing optic pathway, but is not essential for intraretinal axon pathfinding. (*A*) Double immunofluorescent staining of cultured P0 retinal neurons with antibodies against DSCAM (green) or neurofilaments (red). (*Right*) Boxed region shown at higher power. The white arrowhead indicates the growth cone. (*B*) In situ hybridization for *Dscam* on horizontal and coronal sections through the ventral diencephalon of E12.5 WT embryos. on, optic nerve; asterisk, presumptive chiasm; black arrowheads, presumptive optic tracts. (*C*) Flat-mounted E15.5 WT retina stained with antibodies against neuron-specific β-tubulin to label all retinal axons. The box indicates the region in which confocal images through the optic fiber layer were captured in E15.5 $Dscam^{+/+}$ and $Dscam^{del17/del17}$ retinas (*Right*). (*D*) Schematic illustration of the method used to label small groups of RGC axons and images of labeled RGC axons in dorsal retina of E15.5 $Dscam^{del17/del17}$ WT and mutants. Circles indicate the position of the optic disk. D, dorsal; N, nasal; OD, optic disk; T, temporal; V, ventral. (Scale bars: 200 μm.)

diencephalon (Fig. S1). In contrast, expression of the related gene, *Dscaml1* (15), was not detected in the embryonic retina (5) or along the developing optic pathway (Fig. S1).

DSCAM Is Not Essential for the Guidance of RGC Axons Out of the Eye. Because DSCAM has been implicated as a receptor for netrin-1 (8, 9), a key factor controlling the growth of RGC axons out of the eye (10), we analyzed RGC axon patterning in retinas of E15.5 and E17.5 mice carrying a spontaneous mutation in *Dscam* ($Dscam^{del17}$) (16). Homozygous $Dscam^{del17}$ mice display a 70% reduction in *Dscam* mRNA levels (16) and express low amounts of a truncated protein that is unlikely to be functional (14). On the C57BL/6J background used in this study, $Dscam^{del71/del17}$ mutants appear relatively normal until birth, but die perinatally (16).

We found no defects in $Dscam^{del71/del17}$ mutants in the growth of RGC axons toward or out of the optic disk. Labeling of all RGC axons revealed no obvious defects in axon organization in the retina of $Dscam^{del17/del17}$ mutants (Figs. 1*C* and Fig. S2*A*). Moreover, labeling small groups of axons demonstrated normal targeting and exit of RGC axons at the optic disk (Figs. 1*D* and Fig. S2 *B* and *C*). Identical results were obtained using a second *Dscam* mutant allele ($Dscam^{2J}$) that we have confirmed to be protein-null (14) (Fig. S3*A*). These findings demonstrate that DSCAM is not essential for the netrin-dependent process of exiting the eye, in agreement with previous analyses of mice carrying a targeted null mutation in *Dscam* ($Dscam^{-/-}$) that failed to identify a critical requirement for DSCAM in the netrin-induced outgrowth and guidance of spinal commissural axons (11).

Evidence that DSCAM is a netrin-1 receptor has come from binding studies and temporal disruption of DSCAM function using siRNA-knockdown and dominant-negative constructs (8, 9). Studies of other putative netrin-signaling components also have found functional differences following acute pharmacologic- or siRNA-induced knockdown compared with genetic loss of function (17, 18). Thus, future studies may examine whether netrin-signaling is exquisitely sensitive to acute down-regulation of potentially redundant proteins or can compensate for the longer-term loss of signaling components that occurs in genetic null mutants. However, redundancy of DSCAM with DCC, a known netrin-1 receptor, has been excluded, at least for spinal commissural neurons (11).

More RGC Axons Are Present at the Optic Chiasm of *Dscam* Mutants, but Growth Toward Visual Targets Is Impaired. Because DSCAM has been well characterized as a homophilic binding molecule (19, 20) and is expressed both by RGCs and bordering the developing optic pathway, we next asked whether DSCAM regulates RGC growth from the eye toward visual brain targets. The number of RGCs is significantly increased in postnatal $Dscam^{del17/del17}$ retinas (5). Quantitation revealed a significant increase in RGCs also at embryonic stages (Fig. S4 *A*–*C*), likely driven by increased cell production (Fig. S4 *A*, *B*, and *D*) rather than reduced cell death (Fig. S4 *A*, *B*, and *E*). Associated with this increase in RGC number, was a significant increase in the number of RGC axon bundles at the optic chiasm of $Dscam^{del17}$ mutants. Following labeling with DiI of all axons from one eye of E13.5 embryos, more than twice as many RGC axon bundles were labeled in the ipsilateral optic tract of E13.5 $Dscam^{del17/del17}$ mutants compared with stage-matched littermates (Fig. 2 *A* and *B*). At later stages, the width of the ipsilateral optic tract was increased significantly, consistent with a sustained increase in the number of RGC axons (Fig. S5 *A* and *B*). Similar changes in the size of the ipsilateral optic tract were found in $Dscam^{2J}$ mutants (Fig. S3*B*). There was also a trend toward an increase in the number of RGC axons projecting to the contralateral eye in $Dscam^{del17/+}$ and $Dscam^{del17/del17}$ embryos compared with WT littermates (Fig. S5 *C*–*E*).

Although we found that more RGC axons reached the optic chiasm of $Dscam^{del17/del17}$ mutants, extension of these axons into the dorsal thalamus was severely impaired. In the same DiI-labeled embryos used for the chiasm studies, the ipsilateral optic tracts were significantly shorter in $Dscam^{del17/del17}$ mutants compared with stage-matched WT littermates at all ages examined (Fig. 2 *C* and *D*). The number of RGC axon bundles in the ipsilateral dorsal thalamus was also decreased significantly (Fig. 2 *E* and *F*). The length of the contralateral optic tract of $Dscam^{del17/del17}$ mutants was not significantly different compared with WT (Fig. S5 *F* and *G*), but from E16.5, the number of RGC axon bundles in the contralateral dorsal thalamus was decreased significantly (Fig. 2 *G* and *H*). A reduced number of RGC axons in the dorsal thalamus was also found in E16.5 $Dscam^{2J}$ mutants (Fig. S3*C*). Retrograde labeling of RGCs by placing small crystals of DiI into a consistent site in the dorsal thalamus on one side confirmed that fewer RGC axons reached the dorsal thalamus of $Dscam^{del17/del17}$ embryos compared with WT littermates (Fig. S6). Because the same embryos were used for the analyses of the optic chiasm and tract and more RGC axons were present at the optic chiasm (Fig. 2 *A* and *B*), we consider it highly unlikely that a labeling problem or delay in RGC axonogenesis underlies the stunted appearance of the ipsilateral optic tract in $Dscam^{del17}$ mutant embryos. The similar

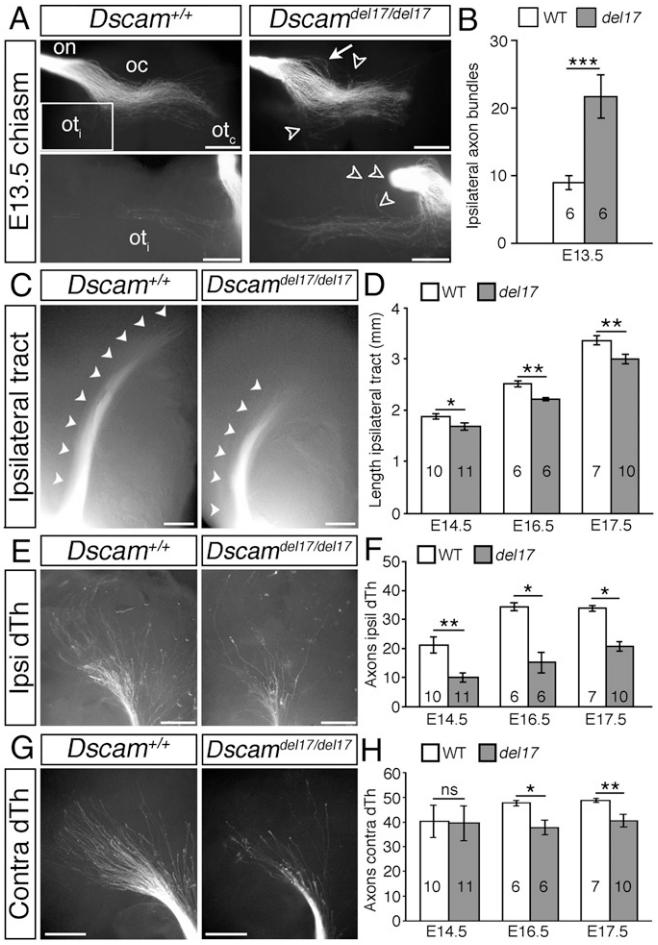

Fig. 2. RGC axon growth through the optic tracts is impaired in *Dscam* mutants. (*A*, *C*, *E*, and *G*) Whole-mount views of anterograde DiI-labeled RGC axons in the optic nerve (on), optic chiasm (oc), and proximal contralateral (ot_c) and ipsilateral (ot_i) optic tracts of E13.5 $Dscam^{del17}$ WT and mutant littermates (*A*) and in the ipsilateral optic tracts (*C*) and ipsilateral and contralateral dorsal thalamus (*E* and *G*) of E16.5 $Dscam^{del17}$ WT and mutant littermates. The boxed region in *A* indicates the region of the ipsilateral optic tract shown at higher power in the lower panels. White arrows indicate defasciculated axons in the optic nerve; open arrowheads, straying axons. (*A*) Ventral views. (*C*, *E*, and *G*) Side views following removal of the cortex. (*B*, *D*, *F*, and *H*) Mean ± SEM number of axon bundles in the ipsilateral optic tract of E13.5 $Dscam^{del17}$ WT and mutant (del17) littermates (*B*), and ipsilateral optic tract length (*D*) and number of axon bundles in the ipsilateral (*F*) and contralateral (*H*) dorsal thalamus (dTh) of E14.5–E17.5 $Dscam^{del17}$ WT and mutant littermates. Analyses were performed blinded to genotype. Numbers on bars indicate the numbers analyzed. $*P < 0.05$; $**P < 0.01$; $***P < 0.001$; ns, not significant. (Scale bars: 250 μm.)

lengths of the contralateral tracts in $Dscam^{del17/del17}$ mutants and WT littermates (Fig. S5 *F* and *G*) also was inconsistent with a developmental delay or significant reduction in brain size in the mutants. The morphology and patterning of the ventral diencephalon of the mutants also appeared relatively normal. The organization of the SSEA-1–positive neurons located posterior to the chiasm and RC2-positive radial glia (21) was similar in $Dscam^{del17/del17}$ mutants and WT littermates (Fig. S7*A*). The expression of *ephrinB2*, *Vegfa*, and *Nrcam*, important for the divergent growth of RGC axons at the chiasm midline (22–24), and *Slit1*, which helps keep RGC axons from straying from their normal pathway (25), also appeared similar in WT and mutants (Fig. S7*B*). Taken together, these findings are consistent with a role for DSCAM in promoting the growth or guidance of RGC axons through the optic tracts.

DSCAM Is Required for Growth and Fasciculation, but Not Guidance, of RGC Axons. Imaging of the optic tracts in whole mounts or sections revealed no significant defects in the path followed by RGC axons as they extended through the optic tracts (Fig. 3*A*). A small number of RGC axons in the optic tracts of $Dscam^{del17/del17}$ mutants projected orthogonally to the normal direction of growth (Fig. 3*A*). At the optic chiasm, we also found small numbers of RGC axons that had strayed from their normal path in the optic nerve, anterior to the optic chiasm and the proximal optic tract (Fig. 2*A*). However, the small number of these aberrant axons does not likely account for the substantial reduction in RGC axons reaching the dorsal thalamus.

Straying of axons in the optic nerve, chiasm, and tract of mice lacking Secreted frizzled-related proteins ($Sfrp1^{-/-}$ and $Sfrp2^{-/-}$) has been attributed, at least in part, to changes in axon fasciculation (26). To test whether DSCAM modulates RGC axon fasciculation, we determined the mean axon bundle width from cultured E14.5 $Dscam^{del17/del17}$ mutant or WT retinal explants (Fig. 3 *B* and *C*). A similar approach has been used to investigate the role of *Sfrp*s (26) and Slit/Robo signaling (27) in modulating axon fasciculation. Axon bundles from $Dscam^{del17/del17}$ retinal explants were significantly thinner than axon bundles from WT explants, and this was true for both presumptive ipsilaterally and contralaterally projecting axons (Fig. 3 *B* and *C*). These findings are consistent with a role for DSCAM in promoting RGC axon fasciculation, and suggest that disrupted axon fasciculation contributes to the straying of RGC axons in $Dscam^{del17/del17}$ mutants.

Although we cannot exclude the possibility that the significant increase in RGC number contributes to the disorganized appearance of the optic pathway in $Dscam^{del17/del17}$ mutants, we consider this unlikely. Mice with defective naturally occurring cell death do not exhibit an increase in RGC number embryonically (Fig. S8 *A* and *B*) (28); however, there is a natural, bimodal variation in RGC number in different strains of mice (29) driven by differences in RGC production (30). No significant differences in chiasm organization in mice on different genetic backgrounds have been reported, however (22, 23, 25, 31, 32) (Fig. S8*C*). Moreover, fasciculation defects of RGC dendrites in *Dscam* mutants can occur independently of increased cell number (6).

We considered the possibility that RGC axons fail to reach the dorsal thalamus because they stall along the optic tracts; however, we found no evidence for accumulation of growth cones within the optic tracts (Figs. 2 *E* and *G* and 3*A*). Moreover, comparison of the length of the ipsilateral optic tract and number of axon bundles within the ipsilateral dorsal thalamus at different ages demonstrated that RGC axons continued to grow in *Dscam* mutants (Fig. 2 *D* and *F*) and ultimately reached their targets (Fig. S9) (33). These findings are consistent with DSCAM providing permissive, but not guidance, signals that promote extension of RGC axons from, but not toward, the optic chiasm.

A similar, spatially restricted requirement for DSCAM in promoting axon extension has been reported for *Drosophila* mechanosensory neurons. In the absence of Dscam1, mechanosensory neurons grow normally into the CNS, but then extension is severely impaired (34). The differential requirement for DSCAM in growth of RGC axons toward and away from the optic chiasm may reflect redundancy with other signals that promote the growth of RGC axons toward the optic chiasm, or a switch in growth cone sensitivity. Further experiments are needed to distinguish between these possibilities.

Morphology of RGC Axon Growth Cones Is Altered in $Dscam^{del17/del17}$ Mutants. In *Drosophila Dscam1* mutants, the impaired extension of mechanosensory axons is associated with changes in growth cone morphology. Growth cones of mutant axons are less complex and have abnormally dense and short filopodia compared with WT axons (35). Analysis of growth cone morphology in the optic tracts of E14.5 $Dscam^{del17/del17}$ mutants and WT littermates revealed a similar loss of growth cone complexity in the mutants (Fig. 3 *D* and *E*). Growth cones were characterized as having either a simple, torpedo-like morphology (longer than wide, with few filopodia) or

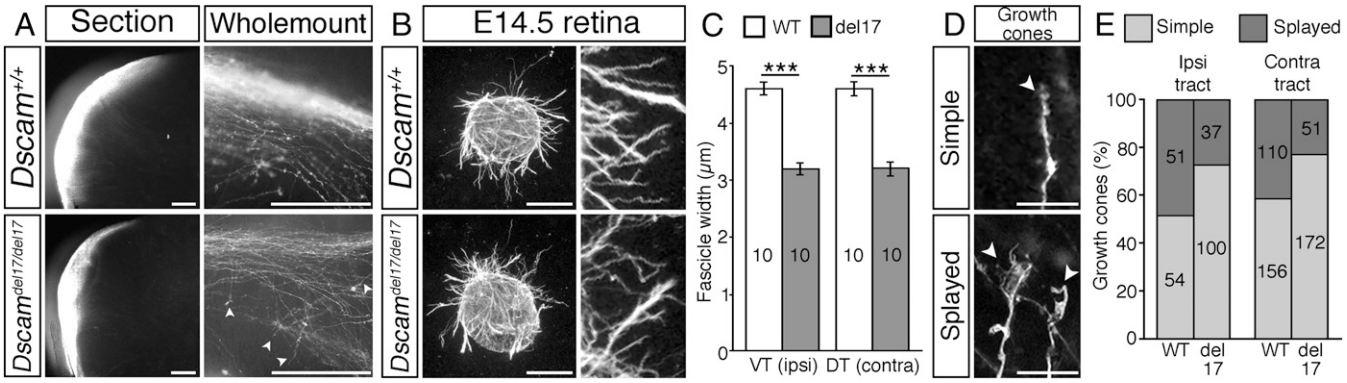

Fig. 3. DSCAM modulates RGC axon fasciculation and growth cone morphology. (*A*) Coronal sections at the level of the optic tracts and whole-mount views of the ipsilateral optic tract of anterograde DiI-labeled *Dscam*^{del17} WT and mutant littermates. Sections, E17.5 embryos; whole mounts, E14.5 embryos. White arrowheads indicate straying axons. (*B*) E14.5 retinal explants from *Dscam*^{del17} mutant and WT littermates cultured in collagen gels for 24 h and stained with antibodies against neuron-specific β-tubulin. (*Right*) Higher-magnification images of the axon bundles. (*C*) Mean ± SEM axon bundle width of *Dscam*$^{+/+}$ and *Dscam*$^{del17/del17}$ retinal axons. Results are the mean from four independent experiments analyzed blinded to genotype. (*D*) DiI-labeled simple and splayed growth cones (white arrowheads) in the ipsilateral optic tract of E14.5 WT embryos. (*E*) Percentage of simple and splayed growth cones in the ipsilateral and contralateral optic tracts of E14.5 *Dscam*^{del17} mutants and WT littermates. Analyses were performed blinded to genotype. Numbers on the bars indicate the numbers analyzed. ***$P < 0.001$. (Scale bars: 250 μm in *A* and *B*; 25 μm in *D*.)

splayed morphology (wider than long with several filopodia; Fig. 3*D*). In both the ipsilateral and contralateral optic tract of *Dscam*$^{del17/del17}$ mutants, a greater percentage of growth cones had simple morphologies compared with WT littermates (Fig. 3*E*). Both in vitro and in vivo reductions in the number of growth cone filopodia decrease the rate of axon outgrowth (36, 37); thus, the reductions in growth cone complexity in *Dscam* mutants may contribute directly to the reduced axon extension in the murine optic tract.

DSCAM Promotes RGC Axon Outgrowth in Vitro. Because axon–axon interactions play an important role in controlling the rate of growth along the developing optic pathway (38), defasciculation could underlie the reduced growth of RGC axons in the absence of DSCAM. Alternatively, DSCAM expressed along the optic pathway may act directly on the RGC growth cones to increase the rate of axon extension. These possible mechanisms are not mutually exclusive and could act together to determine the overall rate of axon outgrowth. To test whether DSCAM provides growth-promoting signals to RGC axons, we cultured E14.5 retinal explants in collagen gels seeded with control or DSCAM-producing cells. In this assay, RGC axons grow among the cells that are dispersed throughout the collagen. Culturing of *Dscam*$^{+/+}$ explants with DSCAM-producing cells induced a significant increase in the extent of axon outgrowth of both presumptive ipsilateral (ventrotemporal) and contralateral (dorsotemporal) RGCs compared with cultures containing control cells (Fig. 4 *A* and *B*).

We next asked whether DSCAM is required in RGC axons, as well as the environment, for promotion of axon outgrowth. In the presence of control cells, the extent of axon outgrowth from WT and *Dscam*$^{del17/del17}$ mutant retinal explants was similar (Fig. 4 *A*–*D*); however, in cultures containing *Dscam*$^{del17/del17}$ retinal explants, the growth-promoting effect of the DSCAM-producing cells was abrogated completely (Fig. 4 *C* and *D*). We conclude that DSCAM is a potent promoter of RGC axon outgrowth and is required in both RGC axons and the environment for enhanced axon growth, consistent with a homotypic mode of action. The growth-promoting effect of DSCAM occurs not simply from the addition of large adhesion molecules to the cultures; culturing E14.5 WT retinal explants in collagen gels seeded with cells producing the highly related molecule DSCAML1 (15) had no effect on RGC axon outgrowth (Fig. 4 *E* and *F*).

DSCAM is constitutively cleaved from transfected cells and the N-terminal portion shed into the medium (14). This raises the possibility that DSCAM may promote RGC axon outgrowth independently of direct contact with expressing cells. To test this idea, we cocultured WT retinal explants at a short distance (100–300 μm) from clusters of mock- or *Dscam*-transfected cells. We found that the outgrowth of both presumptive ipsilateral and contralateral RGC axons was increased significantly from explants cultured a

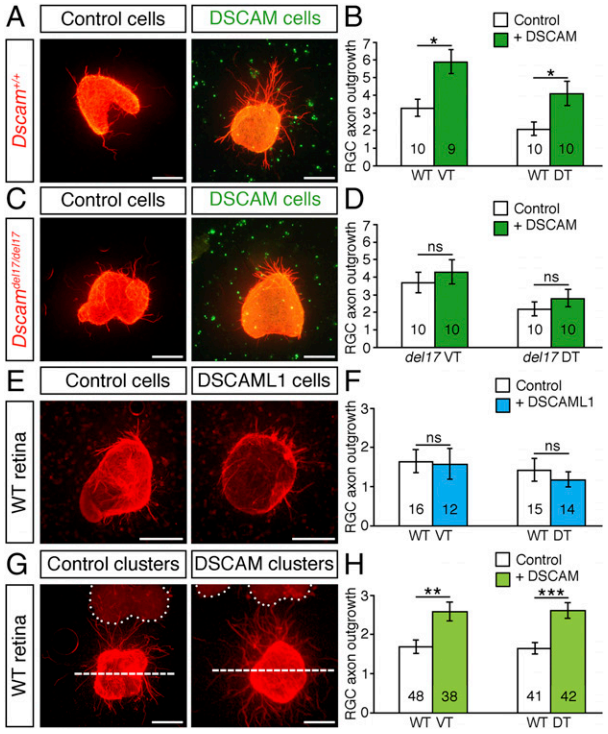

Fig. 4. DSCAM promotes RGC axon outgrowth in vitro. (*A*, *C*, *E*, and *G*) Retinal explants from E14.5 WT (*A*, *E*, and *G*) and *Dscam*^{del17} mutants (*C*) cultured for 24 h in collagen gels seeded with control, *Dscam*-expressing cells (*A* and *C*), *Dscaml1*-expressing cells (*E*), or 100–300 μm from clusters of control or *Dscam*-expressing cells (*G*). Explants were fixed and stained with antibodies against β-tubulin (red) or DSCAM (green). Dotted lines in *G* indicate the outlines of the cell clusters. Outgrowth was quantified in the area above the dashed line. (*B*, *D*, *F*, and *H*) Mean ± SEM axon outgrowth of presumptive ipsilateral (VT) and contralateral (DT) RGCs from WT (*B*, *F*, and *H*) and *Dscam*$^{del17/del17}$ (*D*) retinal explants in the presence of control, DSCAM-producing, or DSCAML1-producing cells. The number of explants analyzed is indicated on the bars. Data are the mean of at least four independent experiments analyzed blinded to genotype and condition. ns, not significant; *$P < 0.05$; **$P < 0.01$; ***$P < 0.001$. (Scale bars: 250 μm.)

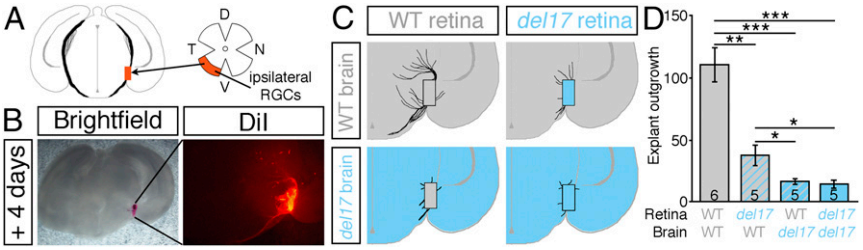

Fig. 5. DSCAM promotes RGC axon outgrowth in situ. (*A*) Schematic diagram of the culture approach. Ventrotemporal retinal explants, containing predominately ipsilaterally projecting RGCs, and brain slices at the level of the optic tract were prepared from E16.5 *Dscam*^{del17} mutant and WT littermates. Retinal explants were cultured on top of the brain slices in different genetic combinations. (*B*) Bright-field and fluorescent (DiI) images of an E16.5 WT retinal explant cultured on a WT brain slice. (*C*) Manual tracing of RGC axons from *Dscam*^{del17} WT (gray) or mutant (blue) retinal explants cultured on WT (gray) or mutant (blue) brain slices. (*D*) Mean ± SEM RGC axon outgrowth from E16.5 *Dscam*^{del17} WT and mutant retinal explants cultured on brain slices from WT and mutant embryos. Numbers on the bars indicate the numbers analyzed. Results are from five independent experiments analyzed blinded to genotype. **P* < 0.05; ***P* < 0.01; ****P* < 0.001.

short distance from DSCAM-producing cell clusters compared with explants cultured at a distance from mock-transfected cells (Fig. 4 *G* and *H*). This finding demonstrates that shed DSCAM can act independently of direct cell–cell contact to modulate cell behavior.

In vitro, we found that DSCAM is a potent growth promoter of both presumptive ipsilateral and contralateral RGC axons (Fig. 4 *A*, *B*, *G*, and *H*); however, in vivo, extension of ipsilateral axons was more severely impaired in *Dscam* mutants (Fig. 2*C–H* and Fig. S5 *F* and *G*). We considered the possibility that a loss of ipsilaterally specified RGCs may contribute to the more severe reduction of ipsilateral projections in *Dscam* mutants, but found no evidence to support this idea. Specification of *Zic2*-positive ipsilaterally projecting RGCs occurred normally in *Dscam*$^{del17/del17}$ mutants (Fig. S4*F*), with a similar number of ZIC2-positive cells present in E16.5 WT and mutant retinas (Fig. S4 *G* and *H*). Contralateral RGC axons may be less sensitive to loss of DSCAM, owing to redundancy with other growth-promoting signals, such as VEGF-A, that act selectively on these axons (22). Alternatively, because ipsilateral axons are selectively sensitive to repellents such as ephrin B2 (24), loss of DSCAM may induce a greater shift toward inhibition in ipsilateral axons. Differential interaction of DSCAM with other potential binding partners, such as Netrin-1 and Slits (8, 9, 39), in ipsilateral vs. contralateral axons also could contribute to the greater dependency of ipsilateral axons on DSCAM for outgrowth in vivo.

DSCAM Is Required in Both RGC Exons and Their Environment for Optimal Axon Outgrowth in Situ. To determine whether in situ DSCAM localized to RGC axons, their environment, or both promotes RGC axon outgrowth, we used a chimeric culture approach adapted from a system used to study corpus callosum development (40). Retinal explants from E16.5 *Dscam*^{del17} WT and mutant littermates were cultured on coronal slices at the level of the optic tract of embryos from the same litters, with explants and slices combined in different genetic combinations (Fig. 5 *A–C*). After 4 d, the cultures were fixed, and DiI was used to label outgrowth from the retinal explants. In cultures of WT retina on WT brain slices, RGC axons extended for some distance from the cultured explants, both toward and away from the optic chiasm (Fig. 5 *B–D*); however, loss of DSCAM from the RGC axons and/or their environment induced a significant decrease in the extent of outgrowth from the cultured explants (Fig. 5 *C* and *D*). Thus, in cultures containing *Dscam*$^{del17/del17}$ retinal explants on *Dscam*$^{+/+}$ brain slices, *Dscam*$^{+/+}$ retinal explants on *Dscam*$^{del17/del17}$ brain slices, or *Dscam*$^{del17/del17}$ retinal explants on *Dscam*$^{del17/del17}$ brain slices, the extent of axon outgrowth from the retinal explants was decreased significantly compared with cultures using only WT tissue (Fig. 5 *C* and *D*). The extent of axon outgrowth from the retinal explants was significantly less in cultures using *Dscam*$^{del17/del17}$ brain slices than in cultures using only mutant retinal tissue (Fig. 5*D*). This could reflect a generally less favorable environment of the mutant brain tissue owing to a reduced number of endogenous RGC axons in the optic tracts (Fig. 2 *C–F*) or to interaction of DSCAM with heterophilic partners in the retina (39).

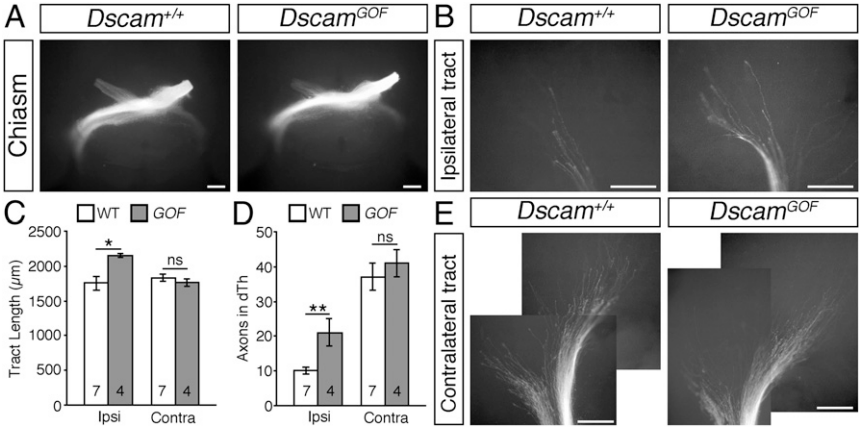

Fig. 6. DSCAM gain of function promotes RGC axon outgrowth in vivo. (*A*, *B*, and *E*) Whole-mount views of anterograde DiI-labeled RGC axons at the optic chiasm (*A*) and in the ipsilateral (*B*) and contralateral (*E*) optic tracts of E14.5 *Dscam*^{GOF} and WT littermates. Panels in E are composite pictures generated by overlying in Adobe Photoshop images captured at overlapping positions along the optic tract. (*C* and *D*) Mean ± SEM optic tract length (*C*) and number of axon bundles in the ipsilateral (ipsi) and contralateral (contra) dorsal thalamus (*D*) of E14.5 *Dscam*^{GOF} (GOF) and WT littermates. Analyses were performed blinded to genotype. Numbers on the bars indicate the numbers analyzed for each genotype. ns, not significant; **P* < 0.05; ***P* < 0.01. (Scale bars: 250 μm.)

***Dscam* Gain of Function Promotes RGC Axon Growth in Vivo.** We used a gain-of-function *Dscam* allele (7) to investigate whether the overexpression of DSCAM affects RGC axon outgrowth in vivo. Anterograde DiI labeling of all axons from one eye of E14.5 $Dscam^{GOF}$ mice and WT littermates demonstrated no significant defects in the growth of RGC axons toward and through the optic chiasm in the transgenic mice (Fig. 6*A*); however, the ipsilateral optic tracts were significantly longer than in WT littermates, with significantly more RGC axon bundles within the dorsal thalamus (Fig. 6 *B–D*). In contrast, the length of the contralateral optic tract and the number of axons bundles in the contralateral dorsal thalamus were not significantly different in $Dscam^{GOF}$ embryos compared with WT littermates (Fig. 6 *C–E*). Thus, gain-of-function experiments induced an opposite phenotype (exuberant growth; Fig. 6 *B–D*) in the ipsilateral optic tract compared with reductions in *Dscam* levels (stunted growth; Fig. 2 *C–F*).

The timing at which RGC axons arrive in the brain correlates with the fidelity of target selection. Early-arriving axons initially innervate multiple targets, followed by pruning of connections to most of these regions. In contrast, later-arriving axons innervate a limited number of targets from the outset (41). By modulating the timing at which RGC axons reach brain targets, DSCAM may contribute to the specificity of brain wiring patterns. Consistent with this idea, *Dscam* gain- and loss-of-function mutants display defects in the eye-specific segregation or RGC axons in the lateral geniculate nucleus (33). Axon overgrowth defects associated with *Dscam* overexpression also have been demonstrated in fragile-X syndrome (42).

Methods

The methodology used in this study is described in detail in *SI Methods*. In brief, gene expression patterns and analyses of axon growth in vivo and in vitro were performed as described previously (22, 25, 43–45). Coculture of retina explants on brain slices was adapted from a method used to study corpus callosum development (40). Animal experiments were performed in accordance with UK Home Office Guidelines and approved by the University of Aberdeen Ethical Review Committee.

ACKNOWLEDGMENTS. We thank Drs. Robert Burgess, Carol Mason, and Eloisa Herrera for helpful discussions; Dr. Thomas Theil for his invaluable advice on the slice culture methods; Francesca Lamb and Emma Smith for technical assistance; and the Institute of Medical Sciences Microscopy and Imaging Facility for assistance with confocal microscopy. This work was supported by a Biotechnology and Biological Sciences Research Council (BBSRC) doctoral training award studentship and a BBSRC project grant (BB/J00815X/1).

1. Erskine L, Herrera E (2014) Connecting the retina to the brain. *ASN Neuro* 6(6): 1759091414562107.
2. Hattori D, Millard SS, Wojtowicz WM, Zipursky SL (2008) Dscam-mediated cell recognition regulates neural circuit formation. *Annu Rev Cell Dev Biol* 24:597–620.
3. Petrovic M, Schmucker D (2015) Axonal wiring in neural development: Target-independent mechanisms help to establish precision and complexity. *BioEssays* 37(9):996–1004.
4. Schmucker D, Chen B (2009) Dscam and DSCAM: Complex genes in simple animals, complex animals yet simple genes. *Genes Dev* 23(2):147–156.
5. Fuerst PG, et al. (2009) DSCAM and DSCAML1 function in self-avoidance in multiple cell types in the developing mouse retina. *Neuron* 64(4):484–497.
6. Fuerst PG, Bruce F, Rounds RP, Erskine L, Burgess RW (2012) Cell autonomy of DSCAM function in retinal development. *Dev Biol* 361(2):326–337.
7. Li S, et al. (2015) DSCAM promotes refinement in the mouse retina through cell death and restriction of exploring dendrites. *J Neurosci* 35(14):5640–5654.
8. Liu G, et al. (2009) DSCAM functions as a netrin receptor in commissural axon pathfinding. *Proc Natl Acad Sci USA* 106(8):2951–2956.
9. Ly A, et al. (2008) DSCAM is a netrin receptor that collaborates with DCC in mediating turning responses to netrin-1. *Cell* 133(7):1241–1254.
10. Deiner MS, et al. (1997) Netrin-1 and DCC mediate axon guidance locally at the optic disc: Loss of function leads to optic nerve hypoplasia. *Neuron* 19(3):575–589.
11. Palmesino E, Haddick PC, Tessier-Lavigne M, Kania A (2012) Genetic analysis of DSCAM's role as a Netrin-1 receptor in vertebrates. *J Neurosci* 32(2):411–416.
12. de Andrade GB, Kunzelman L, Merrill MM, Fuerst PG (2014) Developmentally dynamic colocalization patterns of DSCAM with adhesion and synaptic proteins in the mouse retina. *Mol Vis* 20:1422–1433.
13. de Andrade GB, Long SS, Fleming H, Li W, Fuerst PG (2014) DSCAM localization and function at the mouse cone synapse. *J Comp Neurol* 522(11):2609–2633.
14. Schramm RD, et al. (2012) A novel mouse Dscam mutation inhibits localization and shedding of DSCAM. *PLoS One* 7(12):e52652.
15. Agarwala KL, et al. (2001) Cloning and functional characterization of DSCAML1, a novel DSCAM-like cell adhesion molecule that mediates homophilic intercellular adhesion. *Biochem Biophys Res Commun* 285(3):760–772.
16. Fuerst PG, Koizumi A, Masland RH, Burgess RW (2008) Neurite arborization and mosaic spacing in the mouse retina require DSCAM. *Nature* 451(7177):470–474.
17. Moore SW, et al. (2008) Soluble adenylyl cyclase is not required for axon guidance to netrin-1. *J Neurosci* 28(15):3920–3924.
18. Wu KY, et al. (2006) Soluble adenylyl cyclase is required for netrin-1 signaling in nerve growth cones. *Nat Neurosci* 9(10):1257–1264.
19. Wojtowicz WM, Flanagan JJ, Millard SS, Zipursky SL, Clemens JC (2004) Alternative splicing of Drosophila Dscam generates axon guidance receptors that exhibit isoform-specific homophilic binding. *Cell* 118(5):619–633.
20. Agarwala KL, Nakamura S, Tsutsumi Y, Yamakawa K (2000) Down syndrome cell adhesion molecule DSCAM mediates homophilic intercellular adhesion. *Brain Res Mol Brain Res* 79(1-2):118–126.
21. Marcus RC, Blazeski R, Godement P, Mason CA (1995) Retinal axon divergence in the optic chiasm: Uncrossed axons diverge from crossed axons within a midline glial specialization. *J Neurosci* 15(5 Pt 2):3716–3729.
22. Erskine L, et al. (2011) VEGF signaling through neuropilin 1 guides commissural axon crossing at the optic chiasm. *Neuron* 70(5):951–965.
23. Kuwajima T, et al. (2012) Optic chiasm presentation of Semaphorin6D in the context of Plexin-A1 and Nr-CAM promotes retinal axon midline crossing. *Neuron* 74(4):676–690.
24. Williams SE, et al. (2003) Ephrin-B2 and EphB1 mediate retinal axon divergence at the optic chiasm. *Neuron* 39(6):919–935.
25. Plump AS, et al. (2002) Slit1 and Slit2 cooperate to prevent premature midline crossing of retinal axons in the mouse visual system. *Neuron* 33(2):219–232.
26. Marcos S, et al. (2015) Secreted frizzled related proteins modulate pathfinding and fasciculation of mouse retina ganglion cell axons by direct and indirect mechanisms. *J Neurosci* 35(11):4729–4740.
27. Jaworski A, Tessier-Lavigne M (2012) Autocrine/juxtaparacrine regulation of axon fasciculation by Slit-Robo signaling. *Nat Neurosci* 15(3):367–369.
28. Burne JF, Staple JK, Raff MC (1996) Glial cells are increased proportionally in transgenic optic nerves with increased numbers of axons. *J Neurosci* 16(6):2064–2073.
29. Williams RW, Strom RC, Rice DS, Goldowitz D (1996) Genetic and environmental control of variation in retinal ganglion cell number in mice. *J Neurosci* 16(22):7193–7205.
30. Strom RC, Williams RW (1998) Cell production and cell death in the generation of variation in neuron number. *J Neurosci* 18(23):9948–9953.
31. Sánchez-Arrones L, et al. (2013) Shh/Boc signaling is required for sustained generation of ipsilateral projecting ganglion cells in the mouse retina. *J Neurosci* 33(20): 8596–8607.
32. Williams SE, et al. (2006) A role for Nr-CAM in the patterning of binocular visual pathways. *Neuron* 50(4):535–547.
33. Blank M, et al. (2011) The Down syndrome critical region regulates retinogeniculate refinement. *J Neurosci* 31(15):5764–5776.
34. Chen BE, et al. (2006) The molecular diversity of Dscam is functionally required for neuronal wiring specificity in Drosophila. *Cell* 125(3):607–620.
35. He H, et al. (2014) Cell-intrinsic requirement of Dscam1 isoform diversity for axon collateral formation. *Science* 344(6188):1182–1186.
36. Chien CB, Rosenthal DE, Harris WA, Holt CE (1993) Navigational errors made by growth cones without filopodia in the embryonic Xenopus brain. *Neuron* 11(2): 237–251.
37. McCaig CD (1989) Nerve growth in the absence of growth cone filopodia and the effects of a small applied electric field. *J Cell Sci* 93(Pt 4):715–721.
38. Bak M, Fraser SE (2003) Axon fasciculation and differences in midline kinetics between pioneer and follower axons within commissural fascicles. *Development* 130(20):4999–5008.
39. Alavi M, et al. (2016) Dscam1 forms a complex with Robo1 and the N-terminal fragment of slit to promote the growth of longitudinal axons. *PLoS Biol* 14(9):e1002560.
40. Magnani D, et al. (2014) Gli3 controls corpus callosum formation by positioning midline guideposts during telencephalic patterning. *Cereb Cortex* 24(1):186–198.
41. Osterhout JA, El-Danaf RN, Nguyen PL, Huberman AD (2014) Birthdate and outgrowth timing predict cellular mechanisms of axon target matching in the developing visual pathway. *Cell Reports* 8(4):1006–1017.
42. Sterne GR, Kim JH, Ye B (2015) Dysregulated Dscam levels act through Abelson tyrosine kinase to enlarge presynaptic arbors. *eLife* 4:4.
43. Erskine L, et al. (2000) Retinal ganglion cell axon guidance in the mouse optic chiasm: Expression and function of robos and slits. *J Neurosci* 20(13):4975–4982.
44. Thompson H, Andrews W, Parnavelas JG, Erskine L (2009) Robo2 is required for Slit-mediated intraretinal axon guidance. *Dev Biol* 335(2):418–426.
45. Thompson H, Barker D, Camand O, Erskine L (2006) Slits contribute to the guidance of retinal ganglion cell axons in the mammalian optic tract. *Dev Biol* 296(2):476–484.
46. Fuerst PG, Harris BS, Johnson KR, Burgess RW (2010) A novel null allele of mouse DSCAM survives to adulthood on an inbred C3H background with reduced phenotypic variability. *Genesis* 48(10):578–584.
47. Stacy RC, Wong RO (2003) Developmental relationship between cholinergic amacrine cell processes and ganglion cell dendrites of the mouse retina. *J Comp Neurol* 456(2):154–166.
48. Buffelli M, et al. (2003) Genetic evidence that relative synaptic efficacy biases the outcome of synaptic competition. *Nature* 424(6947):430–434.
49. White FA, Keller-Peck CR, Knudson CM, Korsmeyer SJ, Snider WD (1998) Widespread elimination of naturally occurring neuronal death in Bax-deficient mice. *J Neurosci* 18(4):1428–1439.